Published in final edited form as:
Biomaterials. 2009 January ; 30(3): 354–362. doi:10.1016/j.biomaterials.2008.09.046.

The differentiation of embryonic stem cells seeded on electrospun nanofibers into neural lineages

Jingwei Xie, **Stephanie M. Willerth**, **Xiaoran Li**, **Matthew R. Macewan**, **Allison Rader**, **Shelly E. Sakiyama-Elbert**, and **Younan Xia***
Department of Biomedical Engineering, Washington University, St. Louis, Missouri 63130, USA

Abstract

Due to advances in stem cell biology, embryonic stem (ES) cells can be induced to differentiate into a particular mature cell lineage when cultured as embryoid bodies. Although transplantation of ES cells-derived neural progenitor cells has been demonstrated with some success for either spinal cord injury repair in small animal model, control of ES cell differentiation into complex, viable, higher ordered tissues is still challenging. Mouse ES cells have been induced to become neural progenitors by adding retinoic acid to embryoid body cultures for 4 days. In this study, we examine the use of electrospun biodegradable polymers as scaffolds not only for enhancing the differentiation of mouse ES cells into neural lineages but also for promoting and guiding the neurite outgrowth. A combination of electrospun fiber scaffolds and ES cells-derived neural progenitor cells could lead to the development of a better strategy for nerve injury repair.

1. Introduction

Embryonic stem (ES) cells are pluripotent cells, which have the capacity for continuous self-renewal. Considerable attention has focused on the potential of ES cells or their derivatives in the repairing of nerve injury. It has been demonstrated that the differentiation of ES cells into motor neuron and oligodendrocytes could be induced using various chemical cues [1-3]. McDonald et al. transplanted neural progenitors derived from differentiated mouse ES cells into a rat spinal cord 9 days after traumatic injury [4]. It was shown that the transplant-derived cells survived, differentiated into astrocytes, oligodendrocytes, and neurons, promoting modest functional recovery for the injured rat spinal cord. Keirstead et al. showed that transplantation of oligodendrocyte progenitor cells derived from human ES cells into adult rat spinal cord injuries enhanced remyelination and promoted improvement of motor function [5]. Deshpande et al. explored the potential of motor neurons derived from ES cells to functionally replace those cells destroyed in paralyzed adult rats, demonstrating the potential of restoring functional motor units by ES cells [6]. Recently, Cui *et al.* used a rat sciatic nerve transection model to test the ability of implanted ES cell-derived neural progenitor cells to promote the repair of a severely injured peripheral nerve [7,8]. It was shown that the transplanted ES cells differentiated into myelin-forming cells and offered a potential therapy for severely injured peripheral nerves. These and other studies have clearly established the potential of ES cell transplantation for nerve repair in both central and peripheral nervous system. Unfortunately

* Corresponding author: Younan Xia, Ph.D., Department of Biomedical Engineering, Washington University in St. Louis, Campus Box 1097, One Brookings Drive, Saint Louis, MO 63130, USA. Telephone: +1 314 935 8328; fax: +1 314 935 7448; e-mail: xia@biomed.wustl.edu.

use of ES cell injection techniques has not reliably demonstrated dramatic increases in functional recovery. One hypothesis suggests that muted functional recovery may be a result of improper localization, differentiation, or orientation of ES cells at the site of injection. For this reason many researchers have turned to the use of tissue scaffolds as a means of structuring and organizing ES cell populations *in situ*. To this end, studies have investigated the optimization of fibrin scaffolds for differentiation of murine ES cells into neural lineage cells and the effects of soluble growth factors on ES cell differentiation inside fibrin scaffolds, which could provide a new platform for neural tissue engineering applications (e.g., the treatment of spinal cord injury) [9-11]. Despite some promising results, most of the work is still in an early stage.

Electrospinning is an enabling technology that can be employed to fabricate nanofibers for various biomedical applications, such as drug delivery, biosensing, biocatalysis, and tissue engineering [12]. The fiber diameter can be easily controlled by modulating the operating parameters and physical properties of the solution and the chemical composition can be easily tailored [13]. Electrospun nanofibers can also be functionalized either by blending, encapsulation, or immobilization of bioactive materials (e.g., growth factors and extracellular matrix proteins) to elicit specific biological responses [14]. Furthermore, electrospun nanofibers can be aligned uniaxially with anisotropic properties and they can be utilized to construct microstructured units such as sheets, disks, and tubes [15,16]. Recently, electrospun nanofibers encapsulated with glial derived neurotrophic factor (GDNF) were even used to form nerve conduits for use in repairing peripheral nerve injury over a relatively large gap [17].

In the present study, the major objective is to compare the differentiation of ES cells seeded on randomly and uniaxially aligned poly(ε-caprolactone) (PCL) nanofibers prepared by electrospinning. The effect of topography, using both isotropic and anisotropic properties, on the differentiation of ES cells was examined. A combination of ES cell therapy and nanofibrous scaffold (which can possibly be loaded with growth factors) could provide a better strategy for nerve injury repair.

2. Materials and methods

2.1. Electrospinning of PCL nanofibers

The electrospinning setup and the collector used for fabricating and collecting aligned nanofibers are similar to those used in our previous studies [15]. It consists of five components: syringe pump, syringe, needle, high voltage generator, and collector. The polymer solution used for electrospinning contained 20% PCL (w/v) in a mixed solvent of dichloromethane (DCM) and dimethylformaldehyde (DMF) with a volume ratio of 80:20. Two different collectors, a glass cover slip and a stainless steel frame with an air gap, were employed to collect randomly and uniaxially aligned fibers, respectively. Following electrospinning, the aligned fiber samples were transferred to glass cover slips and then fixed using Silastic Type A Medical Adhesive (Dow Corning Co, Midland, MI, USA). The PCL fibers were sputter-coated with gold before imaging with scanning electron microscope (Nova 200 NanoLab, FEI, Oregon, USA) at an accelerating voltage of 15 kV. Samples prepared for use in cell culture were inserted into a 24-well TCPS culture plate and sterilized via ethylene oxide gas sterilization.

2.2. ES cell culture and embryoid body formation

The protocol for ES cell culture and embryoid bodies (EBs) formation was identical to that described previously [10]. CE3 and RW4 mouse ES cells were obtained from Dr. Gottlieb and cultured in T25 culture flasks coated with a 0.1% gelatin solution (Sigma-Aldrich, St. Louis, MO) in the presence of 1000 U/mL leukemia inhibitory factor (LIF; Chemicon, Temecula,

CA) and 10^{-4} M β-mercaptoethanol (BME; Invitrogen, Grand Island, NY) to maintain their undifferentiated state. Cells were cultured in complete media consisting of Dubecco's modified eagle media (Invitrogen) supplemented with 10% new born calf serum, 10% fetal bovine serum (Invitrogen), and 0.3 mM of each of the following nucleosides: adenosine, guanosine, cytosine, thymidine, and uridine (Sigma-Aldrich), and passaged at a ratio of 1:4 every two days.

Undifferentiated ES cells were induced to form EBs containing neural progenitor cells using the 4-/4+ retinoic acid treatment protocol [18]. ES cells were cultured in 100 mm Petri dishes coated with a 0.1% agar solution (Sigma-Aldrich) in complete media in the absence of LIF and BME for 4 days. Retinoic acid (Sigma-Alrdich) at 500 nM was then added to the complete media for the final 4 days of culture. Media was changed every other day during the eight day process.

2.3. Seeding of EBs and ES cells on PCL fibers scaffolds

One mL of neural basal media containing B27 supplement (Invitrogen) was diluted by 1:50 and added to each well of a 24-well plate (Corning, Corning, NY) containing nanofiber samples. Three EBs were seeded onto the surface of PCL fibers in each well. The media was not changed for the rest of the experiment. In order to investigate the differentiation of ES cells on the surface of PCL fibers without forming EBs, ~10^5 ES cells were transferred from culture flask into each well of 24-well plate and cultured using the 4-/4+ retinoic acid treatment protocol described as above.

2.4. Immunohistochemistry

Immunohistochemical analysis performed to visualize the spatial distribution of cells and neurites. After 14 days of EB culture, each well was washed with 1 mL of phosphate buffer saline (PBS; Invitrogen) and then fixed for 30 min with 400 μL of 3.7% formaldehyde. When necessary, cells were then permeabilized using 400 μL of 0.1% triton-X in PBS for 30 min. Cells were blocked with 400 μL of 5% normal goat serum (NGS; Invitrogen) in PBS for 1 hour and incubated with primary antibody overnight at 4 °C. The following primary antibody dilutions were used to characterize various mature cells found in cultures: Tuj1 (1:500), O4 (1:100), and GFAP (1:40). Following incubation, each well was washed 3 times with PBS for 5 min each. Appropriate secondary antibodies (1:200 dilution) were applied for 1 hour at room temperature. Each well was then washed with PBS and fluorescent images were taken using a QICAM Fast Cooled Mono 12-bit camera (Q Imaging, Burnaby, BC, Canada) attached to an Olympus microsocope with OCapture 2.90.1 (Olympus, Tokyo, Japan).

2.5. Quantitative analysis of neurite extension from cultured EBs

Behavior of neurite populations extending from EBs cultured on PCL nanofiber samples was examined via quantitative analysis of neurite field morphology. A custom-designed computer program, created using MATLAB (MathWorks Inc., Novi, MI, USA), was utilized to analyze fluorescent micrographs of Tuj1-labeled EBs cultured for 14 days on either random or aligned nanofiber samples. Neurite field eccentricity (a measure of directed neurite growth along a given axis) and maximum length of neurite extension (a measure of the rate of neurite growth) were calculated for each EB/sample. Calculations were accomplished by separately fitting the leading edge of the neurite field and the perimeter of the EB cell mass to standard elliptical equation (1) at point (h, k) of the form:

$$\frac{(x-h)^2}{a^2}+\frac{(y-k)^2}{b^2}=1 \quad (1)$$

where *a* and *b* are the ellipse's semimajor and semiminor axes.

Eccentricity of the neurite field was then calculated using the equation (2):

$$\text{Ecc.} = \frac{\sqrt{(a^2 - b^2)}}{a} \quad (2)$$

Where values of a and b were obtained from the elliptical equation fit to the leading edge of the neurite field. Maximum length of neurite extension was then calculated as the greatest distance between the elliptical curve marking leading edge of the neurite field and the elliptical curve marking the boarder of the EB cell mass along a line oriented radially from the center of the EB cell mass.

2.6. Analysis of cell phenotype by flow cytometry

After 14 days of EB culture, the medium was aspirated from each well followed by washing with 1 mL of PBS. Then, 250 μL of trypsin-EDTA (0.25%) (Invitrogen) was added to each well and incubated at 37 °C for 15 min, and 250 μL of complete medium was used to cease the reaction. The cells were removed from each well, centrifuged, and resuspended in PBS.

Extracellular antigen labeling was accomplished using O4 marker (1:100; Chemicon) for oligodendrocytes and SSEA-1 marker (1:25; Chemicon) for undifferentiated ES cells. Cells were incubated in PBS containing 5% NGS for 30 min, followed by applying primary antibody diluted with PBS containing 2% NGS for 1 hour. Cells were then washed twice with PBS prior to addition of the secondary antibody (AlexaFluor 488 goat anti-mouse IgM (1:200; Invitrogen)) diluted with PBS containing 2% NGS, which was applied for 1 hour.

Intracellular antigen labeling was accomplished by fixing cells with PBS containing 1% formaldehyde (Sigma) for 30 min. Cells were permeabilized using 0.1% Triton x-100 (Invitrogen) in PBS for 20 min, followed by blocking in PBS containing 5% NGS for 30 min. Primary antibodies (nestin marker (1:100; Chemicon) for neural precursor, β-tubulin III (Tuj 1) marker (1:1000; Covance, Berkeley, CA) for early neuron, and glia fibrillary acidic protein (GFAP) marker (1:40; Immuostar, Hudson, WI) for astrocytes were diluted with PBS containing 2% NGS and applied to the cells for 1 hour. Cells were washed three times with PBS containing 2% FBS. The secondary antibodies, AlexaFluor 488 goat anti-mouse IgG (1:200; Invitrogen) for detecting nestin and Tuj 1 markers and AlexaFluor 488 goat anti-rabbit IgG (1:200; Invitrogen) for detecting GFAP marker, were diluted with PBS and applied to the cells for 1 hour. After incubation, the cells were washed three times and sorted.

Cellular fluorescence was detected using a FACSCalibur flow cytometry (Becton, and Dickinson Company, Franklin, Lakes, NJ) equipped with an argon laser emission of 488 nm. As a control, cells stained with only the same secondary antibody were used to eliminate nonspecific background staining.

2.7. Cell viability analysis

A live/dead viability/cytotoxicity kit (Invitrogen), consisting of calcein AM and ethidium homodimer-1 (Ethd-1), was used to qualitatively assess cell viability. The intracellular esterase present in live cells converts calcein AM, a cell permeable dye, to calcein, resulting in a bright green fluorescence. EthD-1 can penetrate damaged membranes of dead cells where it binds to nucleic acids, producing intense red fluorescence. Media was removed from each well and samples were washed with PBS. The EBs were incubated for 30 min with 400 μL solution containing 2 μM calcein AM and 4 μM EthD-1 dissolved in PBS, respectively, prior to analysis via fluorescent microscopy.

2.8. Statistical analysis

Mean values and standard deviation were reported. Statistical analysis of eccentricity of neurite field and maximum neurite length was performed using unpaired Student t-Test at a 95% confidence level. Comparative analyses between each phenotype were performed using the Scheffe's F post hoc test by analysis of variance at a 95% confidence level. Three sets of 24-well plates containing nanofiber scaffolds with EB cultures were used to provide enough cells (5000 per sort) for cell phenotype analysis and statistical analysis on the results.

3. Results

3.1. Fabrication of PCL nanofibers

To investigate the topographic effect on the differentiation of ES cells, aligned and random PCL nanofibers were fabricated using electrospinning. Fig. 1, A and B, shows SEM images of aligned and random PCL nanofibers, respectively. The aligned nanofibers were obtained using a metal frame with a void gap as a collector, which was developed by our group [15]. The fiber diameter was around 250 nm. Using this simple setup, PCL nanofibers with diameters ranging from tens of nanometers to several micrometers can be prepared as uniaxially aligned arrays by fine-tuning the conditions for electrospinning.

3.2. CE3 EBs seeded on PCL nanofibers

To initiate differentiation, ES cells were cultured to aggregate into EBs using the 4-/4+ protocol and then seeded onto PCL nanofibers. CE3 cells, which express green fluorescent protein (GFP) under a β-actin promoter, were easily visualized under a fluorescence microscope during culture [19]. Fig. 2 shows fluorescence micrographs of CE3 EBs after seeding on aligned and random PCL nanofibers for 14 days, respectively. Comparison between aligned and random fiber samples demonstrated that cells migrated away from the EB along the long axes of the aligned PCL nanofibers. In contrast, cells cultured on random PCL nanofibers remained more localized to the region of the EB's main body. The inset in Fig.2B shows Tuj1 marker staining which indicates early neurons, suggesting neurites extended along the long axis of the aligned nanofiber samples.

3.3. RW 4 EBs seeded on PCL nanofibers

To determine what mature cell types were present after 14 days of culture, immunostaining was performed using three different markers: Tuj1 (early neurons), O4 (oligodendrocytes), and glia acidic fibrillary protein (GFAP) (astrocytes). Immunohistochemistry confirmed the presence of the mature markers expressed by Rw4 EBs seeded on PCL nanofibrous scaffolds after 14 days (Figs. 3 and 4).

Fig. 3 shows the immunostaining of RW4 EBs after culturing for 14 days on aligned PCL nanofibers. Figures 3A and 3B show the results of the Tuj1 staining. Tuj1 staining is localized to cells which display a clear neuronal phenotype, evidenced by the clear visualization of both cell bodies and extending axonal protrusions. Figures 3C and 3D show the results of staining for O4. Cells immunoreactive to O4, an antibody recognizing oligodendrocyte-specific glycolipid, demonstrated a multipolar morphology characteristic of oligodendrocytes. Figures 3E and 3F show the results of staining for GFAP. Cells expressing the astrocytic marker antigen GFAP exhibited a flat morphology typical of cultured astrocytes. Interestingly, images confirm that neurites extended along the direction of nanofiber alignment. Oligodendrocytes also appeared to migrate along the long axis of aligned fibers, indicating possibility of myelination of extending axons.

Fig. 4 shows the immunostaining of RW4 EBs after culturing on random PCL nanofibers for 14 days. Figures 4A and 4B show the results of the Tuj1 staining. Cells migrating out of the

EBs and staining positive for Tuj1 possessed long neurotic axon-like processes characteristic of neuronal cells. Figures 4C and 4D show the results of staining for O4. Cells immunoreactive to O4 presented a multipolar morphology which was typical for oligodendrocytes. Figures 4E and 4F show the results of staining for GFAP. Cells which migrated out of the EBs and stained positive for the astrocytic marker antigen GFAP had a star-like morphology, characteristic of astrocytes. Most importantly, neurites appeared to extend in all the directions from the EB's main body in a random fashion. The random distribution and direction of extending neurite was dramatically different then that demonstrated on aligned PCL nanofiber samples. Also, oligodendrocytes and astrocytes migrated randomly to the surrounding region of EBs. Furthermore, more astrocytes seemed to be present around EBs cultured on random fibers than those on aligned fibers.

Quantitative analysis of neurite field morphology was performed using a custom-designed MATLAB program. Neurite field eccentricity and maximum neurite length were calculated for EBs cultured on both random and aligned nanofiber samples (Fig. 5). Neurite fields extending from EBs cultured on aligned nanofiber samples exhibited a significantly higher degree of eccentricity compared to those extending from EBs cultured on random fibers. Closer inspection of analyzed fluorescent micrographs demonstrated that the major axis of the elongated neurite fields found on aligned nanofiber samples correspond with the axis of both nanofiber alignment and individual neurite length. In contrast, individual neurites in less eccentric neurite fields found on random nanofiber samples did not exhibit any type of alignment and generally extended radially from the EB cell mass. Together, these observations suggest that aligned nanofiber surfaces are capable of directing and aligning populations of extending neurites, and that neurite field eccentricity serves as an accurate estimation of individual neurite behavior. In addition, the maximum length of neurites projecting from EBs cultured on aligned nanofibers samples was significantly higher, ~500 μm longer, than that of neurites projecting from EBs cultured on random nanofibers. Aligned nanofiber samples may, therefore, be capable of enhancing the rate of neurite extension as well as the direction.

Flow cytometry was used to quantify the presence of differentiated cell phenotypes on nanofiber surfaces. Fig. 6 shows the results of cell phenotype analysis. Percentage of SSEA-1 positive cells decreased from around 96% (undifferentiated ES cells) to 60% (EB) after 4-/4+ protocol treatment, indicating that the cells were undergoing differentiation during the formation of EB, which agreed well with previous report [10]. And it further decreased to 40% and 38% for EB cultured on aligned and random nanofiber samples, respectively. Percentages of SSEA-1 and nestin-positive cells were comparable between populations isolated from both aligned and random nanofibers. The number of cells expressing Tuj1 and O4 markers was slightly higher on aligned fibers than those on random fibers. Cells cultured on aligned fiber samples also demonstrated lower number numbers of GFAP-positive cells in comparison to populations isolated from random fiber samples. These results imply that the microenvironment of alignment may have discouraged the development of astrocytes, which is much favorable due to the glial scar formation by astrocytes during spinal cord injury. These findings also suggest that seeding EBs onto PCL nanofibrous scaffolds could potentially provide an approach to generating neural cells to replace those lost due to spinal cord injury.

Fig. 7 shows representative images of live/dead assay staining. Fig. 7A shows live cell present in intact EBs on aligned nanofiber samples. It is noted that the live cells migrated along the direction of fiber alignment. Fig. 7B shows dead cells present in intact EBs. Dead cells were not observed in the regions outside of the main body of the EB. Fig. 7C shows that live cells were present in intact EBs and in the surrounding region. These images also confirm that many live cells migrated from the main body to peripheral areas. Fig. 7D shows dead cells present in an intact EB and few dead cells appeared in the circumambient region except for main body.

3.4. CE3 cells seeded onto PCL nanofibers without forming EBs

Through above studies, it is clear that ES cells via formation of EBs treated with retinoic acid seeded onto PCL nanofibers were capable of differentiatiing into neural lineage cells and extending neurites across nanofibers substrates. In order to investigate the effect of PCL nanofiber matrix on the differentiation of ES cells without forming EBs, CE3 cells were seeded directly onto PCL nanofibers, induced by retinoic acid, and then cultured in neural basal media with B27 as a supplement. Culture ES cells were found to form aggregates on both aligned and random PCL nanofibers. After 14 days, immunostaining was performed against the neuronal marker Tuj1. Fig. 8 shows Tuj1-positive cells, suggesting neuronal differentiation of CE3 cells seeded on PCL nanofibers. Figures 8A and 8B show the green fluorescent images of CE3 cells owing to their expression of green fluorescent protein. Figures 8C and 8D show immunostaining with the neuronal marker Tuj1, showing neuronal differentiation. Neurite outgrowth can be clearly observed. Also, it was demonstrated that neurite extension was guided by the direction of nanofiber alignment. Figures 8 E and 8F were superimposed images of Figures 8A and 8C and Figures 8B and 8D, respectively, suggesting that a portion of the cells had differentiated into neurons.

4. Discussion

ES cells can be induced to become specific lineages by chemical cues [15,20]. However, it has been a great challenge to control cell proliferation and differentiation into higher order structures for delivering and promoting their efficient engraftment, which could provide potential functional tissue constructs for direct implantation [21,22]. Enhanced control of ES cells differentiation into neural lineage cells is an important feature in designing functional tissue constructs for use in repairing neurological injuries. In the present study, characterization of ES cells culture on both random and aligned electrospun PCL nanofibers demonstrated the important role of material topology in ES cell differentiation. When EBs cultured onto PCL nanofibers, they were capable of differentiating into mature neural lineage cells including neurons, oligodendrocytes, and astrocytes. Neural precursors were also observed, which have potential to differentiate into mature neural cells. The presence of neural precusor cells is very desirable for the treatment of spinal cord injury.

ES cell differentiation has been demonstrated to be strongly affected by interactions with external physical and chemical stimuli, including the topography and composition of extracellular matrix [23,24]. The present study demonstrated that aligned nanofiber substrates could discourage the differentiation of ES cells into astrocytes, which is much desirable in therapies targeting spinal cord injuries, as they may limit the possible glia scar formation. Similar findings were reported for self-assembled, laminin-derived peptide nanofibers, as the substrates could also minimize astrocytic differentiation [25].

Contact guidance of neurite outgrowth has been investigated using surface patterning techniques such as lithography and microcontact printing [26-28]. It was shown that the neural processes preferred to grow on ridge edges and elevations on surfaces rather than in grooves. Also, the neural stem cell line C17.2 was examined on electrospun fibers for neural tissue engineering applications [29]. It was demonstrated that the direction of neural stem cell elongation and its neurite outgrowth was parallel to the direction of fiber alignment for aligned scaffolds. The rate of neural stem cell differentiation was higher on nanofibers than that on microfibers and it was independent of the fiber alignment. In the present study, we also demonstrated that the aligned electrospun fibers could guide the neurite outgrowth generated by the differentiated neurons. The benefits of alignment might be valuable for nerve injury repair by helping to restore some of the cellular architecture that is lost after injury.

Recent studies suggested that transplantation of ES cells could also be used as a means of treating peripheral nerve injuries and possibly spinal cord injuries [7,8]. The present study demonstrated that aligned nanofibers are capable of directing and guiding neurite extension over significant distances. Hence, a combination of ES cell therapy and nerve conduits composed of aligned nanofibers could provide a better approach to peripheral nerve repairing than direct injection of cells into the injury site because the scaffolds can provide a more hospitable environment for cell survival and trophic support for seeded ES cells [30]. Besides, electrospun fibers can be easily functionalized through encapsulation or immobilization of growth factors or extracellular matrix proteins combining drug delivery systems, which could be used to further direct ES cell differentiation [31]. The addition of growth factors could help to enhance differentiation of ES cells into neurons, neural precursors, and oligodendrocytes [10,11].

Most of the current ES cell culture protocols use of EB formation to achieve neuronal differentiation. Smith et al. demonstrated the conversion of ES cells into neuroectodermal precursors in adherent monoculture [32]. Here, we demonstrated the neuronal differentiation of CE3 cells seeded directly onto PCL nanofibers without formation of EBs. The successful differentiation of disassociated ES cells suggests a new route to the fabrication of higher ordered neural tissue constructs. Further studies will be concentrated on *in vivo* applications of combined systems incorporating nanofiber scaffold and ES cells-derived neural progenitor cells for nerve injury repair.

5. Conclusions

We have demonstrated that ES cells can be induced to differentiate into specific neural lineages, specifically neurons, oligodendrocytes, and astrocytes, when seeded onto electrospun fibrous scaffolds. Aligned nanofibers prepared by electrospinning could not only enhance the differentiation into neural lineages but also direct the neurite outgrowth. The present study may provide a new platform that combines nanostructured scaffolds and ES cell therapy for nerve injury repair.

Acknowledgements

This work was supported by a 2006 NIH Director's Pioneer Award (3DPOD000798) and start-up funds from the Washington University in St. Louis. Our warm thanks to Professor David I. Gottlieb at Department of Anatomy and Neurobiology, Washington University, St. Louis) for providing us with stem cell lines. X.L. is a visiting Ph.D. student from the School of Materials Science and Engineering, Tianjin University, Tianjin, China and was partially supported by the National Council of Scholarship.

References

1. Wichterle H, Lieberam I, Porter JA, Jessell T. Directed differentiation of embryonic stem cells into motor neurons. Cell 2002;110:385–97. [PubMed: 12176325]
2. Miles GB, Yohn DC, Wichterle H, Jessell TM, Rafuse VF, Brownstone RM. Functional properties of motorneurons derived from moue embryonic stem cells. J Neurosci 2004;24:7848–58. [PubMed: 15356197]
3. Liu S, Qu Y, Stewart TJ, Howard MJ, Chakrabortty S, Holekamp TF, et al. Embryonic stem cells differentiate into oligodendrocytes and myelinate in culture and after spinal cord transplantation. PNAS 2000;97(11):6126–31. [PubMed: 10823956]
4. McDonald JW, Liu XZ, Qu Y, Liu S, Mickey SK, Turetsky D, et al. Transplanted embryonic stem cells survive, differentiate and promote recovery in injured rat spinal cord. Nature Med 1999;5(12): 1410–2. [PubMed: 10581084]
5. Keirstead HS, Nistor G, Bernal G, Totoiu M, Cloutier F, Sharp K, et al. Human embryonic stem cell-derived oligodendrocyte progenitor cell transplants remyelinate and restore locomotion after spinal cord injury. J Neurosci 2005;25(19):4694–705. [PubMed: 15888645]

6. Deshpande DM, Kim YS, Martinez T, Carmen J, Dike S, Shats I, et al. Recovery from paralysis in adult rats using embryonic stem cells. Ann Neurol 2006;60:32–44. [PubMed: 16802299]
7. Cui L, Jiang J, Wei L, Zhou X, Fraser JL, Snider BJ, et al. Transplantation of embryonic stem cells improves nerve repair and functional recovery after severe sciatic nerve axotomy in rats. The FASEB J 2007;21:1–11.
8. Cui L, Jiang J, Wei L, Zhou X, Fraser JL, Snider BJ, et al. Transplantation of embryonic stem cells improves nerve repair and functional recovery after severe sciatic nerve axotomy in rats. Stem Cells 2008;26(5):1356–65. [PubMed: 18308951]
9. Willerth SM, Arendas KJ, Gottlieb DI, Sakiyama-Elbert SE. Optimization of fibrin scaffolds for differentiation of murine embryonic stem cells into neural lineage cells. Biomaterials 2006;27:5990–6003. [PubMed: 16919326]
10. Willerth SM, Faxel TE, Gottlieb DI, Sakiyama-Elbert SE. The effects of soluble growth factors on embryonic stem cell differentiation inside of fibrin scaffolds. Stem Cells 2007;25(9):2235–44. [PubMed: 17585170]
11. Willerth SM, Rader A, Sakiyama-Elbert SE. The effect of controlled growth factor delivery on embryonic stem cell differentiation inside fibrin scaffolds. Stem Cell Research. 2008in press
12. Dzenis Y. Spinning Continuous Fibers for Nanotechnology. Science 2004;304:1917–19. [PubMed: 15218134]
13. Li D, Xia YN. Electrospinning of nanofibers: reinventing the wheel? Adv Mater 2004;16(14):1151–70.
14. Liang D, Hsiao BS, Chu B. Functional electrospun nanofibers scaffolds for biomedical applications. Adv Drug Del Rev 2007;59:1392–412.
15. Li D, Wang YL, Xia YN. Electrospinning of polymeric and ceramic nanofibers as uniaxially aligned arrays. Nano Lett 2003;3(8):1167–71.
16. Li D, Wang YL, Xia YN. Electrospinning nanofibers as uniaxially aligned arrays and layer-by-layer stacked films. Adv Mater 2004;16(4):361–66.
17. Chew SY, Mi R, Koke A, Leong KW. Aligned protein-polymer composites fibers enhance nerve regeneration: a potential tissue-engineering plateform. Adv Funct Mater 2007;17:1288–96. [PubMed: 18618021]
18. Bain G, Kitchens D, Yao M, Huettner JE, Gottlieb DI. Embryonic stem cells express neuronal properties in vitro. Dev Biol 1995;168(2):342–57. [PubMed: 7729574]
19. Adams LD, Choi L, Xian HQ, Yang A, Sauer B, Wei L, et al. Double *lox* targeting for neural cell transgenesis. Mol Brain Res 2003;110(2):220–33. [PubMed: 12591158]
20. Schuldiner M, Yanuka O, Itskovitz-Eldor J, Melton DA, Benvenisty N. Effects of eight growth factors on the differentiation of cells derived from human embryonic stem cells. PNAS 2000;97(21):11307–12. [PubMed: 11027332]
21. Levenberg S, Huang NF, Lavik E. Differentiation of human embryonic stem cells on three-dimensional polymer scaffolds. PNAS 2003;100(22):12741–46. [PubMed: 14561891]
22. Mooney DJ, Vandenburgh H. Cell delivery mechanisms for tissue repair. Cell Stem Cell 2008;2(3):205–13. [PubMed: 18371446]
23. Dawson E, Mapili G, Erickson K, Taqvi S, Roy K. Biomaterials for stem cell differentiation. Adv Drug Del Rev 2008;60:215–28.
24. Hwang NS, Varghese S, Elisseeff J. Controlled differentiation of stem cells. Adv Drug Del Rev 2008;60:199–214.
25. Silva GA, Czeisler C, Niece KL. Selective differentiation of neural progenitor cells by high-epitope density nanofibers. Science 2004;303:1352–55. [PubMed: 14739465]
26. Johansson F, Carlberg P, Danielsen N, Montelius L, Kanje M. Axonal outgrowth on nanoimprinted patterns. Biomaterials 2006;27:1251–58. [PubMed: 16143385]
27. Cecchini M, Bumma G, Serresi M, Beltram F. PC12 differentiation on biopolymer nanostructures. Nanotechnology 2007;18:505103.
28. Philipsborn ACV, Lang S, Bernard A, Loeschinger J, David C, Leh D. Microcontact printing of axon guidance molecules for generation of graded patterns. Nature Protocol 2006;1(3):1322–28.

29. Yang F, Murugan R, Wang S, Ramakrishna S. Electrospinning of nano/micro scale poly($_L$-lactic acid) aligned fibers and their potential in neural tissue engineering. Biomaterials 2005;26:2603–10. [PubMed: 15585263]

30. Willerth SM, Sakiyama-Elbert SE. Cell therapy for spinal cord injury. Adv Drug Del Rev 2008;60:263–76.

31. Willerth SM, Sakiyama-Elbert SE. Approaches to neural tissue engineering using scaffolds for drug delivery. Adv Drug Del Rev 2007;59:325–38.

32. Ying QD, Stavridis M, Driffiths D, Li M, Smith A. Conversion of embryonic stem cells into neuroectodermal precursors in adherent monoculture. Nature Biotech 2003;21:183–86.

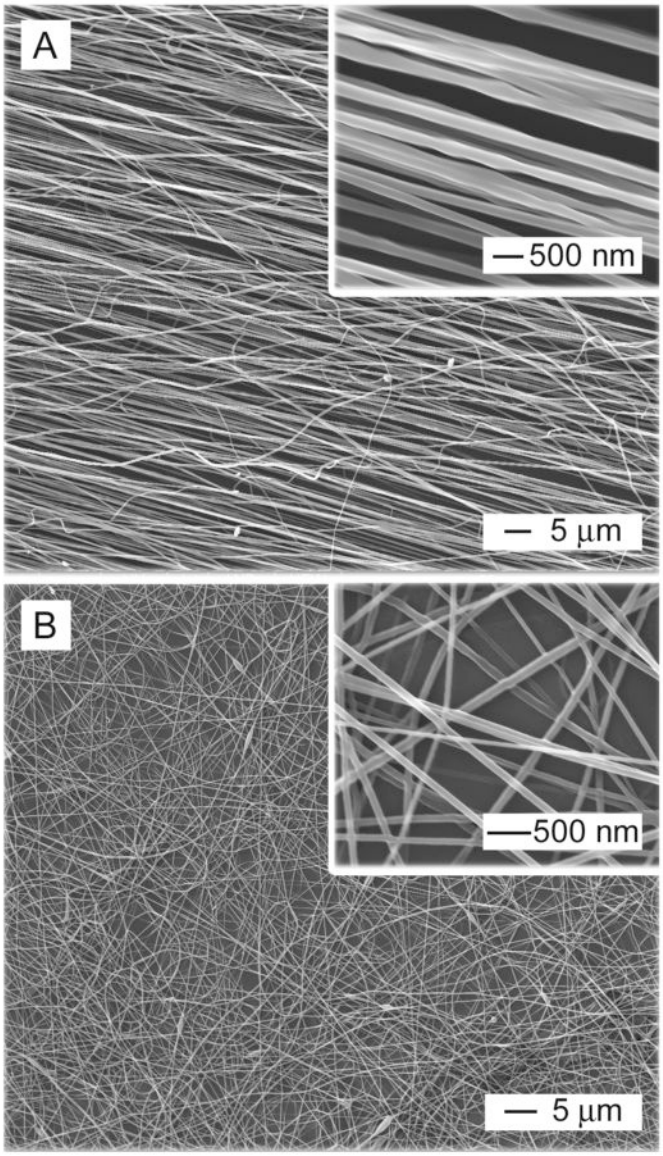

Fig.1.
SEM images of (A) aligned PCL nanofibers prepared by electrospinning and (B) randomly oriented PCL nanofibers.

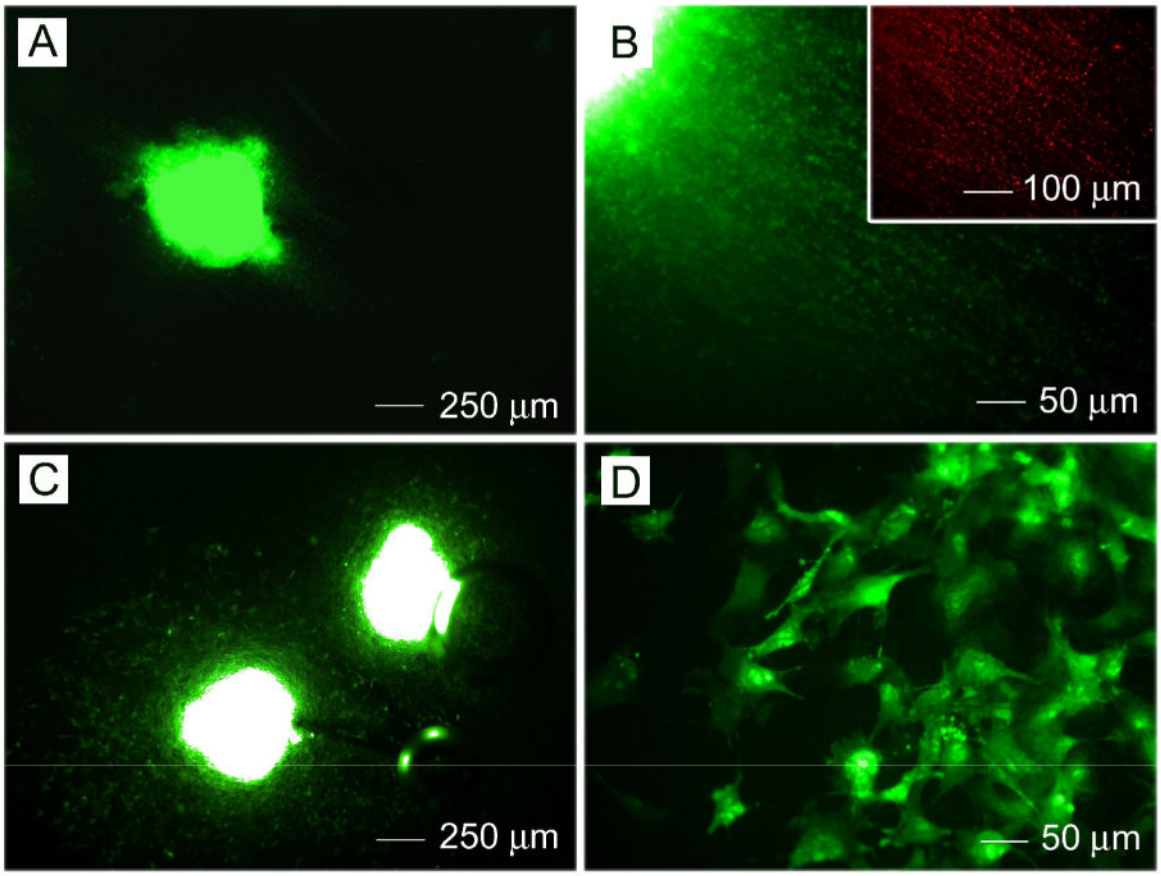

Fig.2.
Fluorescence microscopy images of CE3 embryoid bodies after seeding onto (A, B) aligned and (C, D) randomly oriented PCL nanofibers for 14 days. Inset: staining with neuron marker Tuj1.

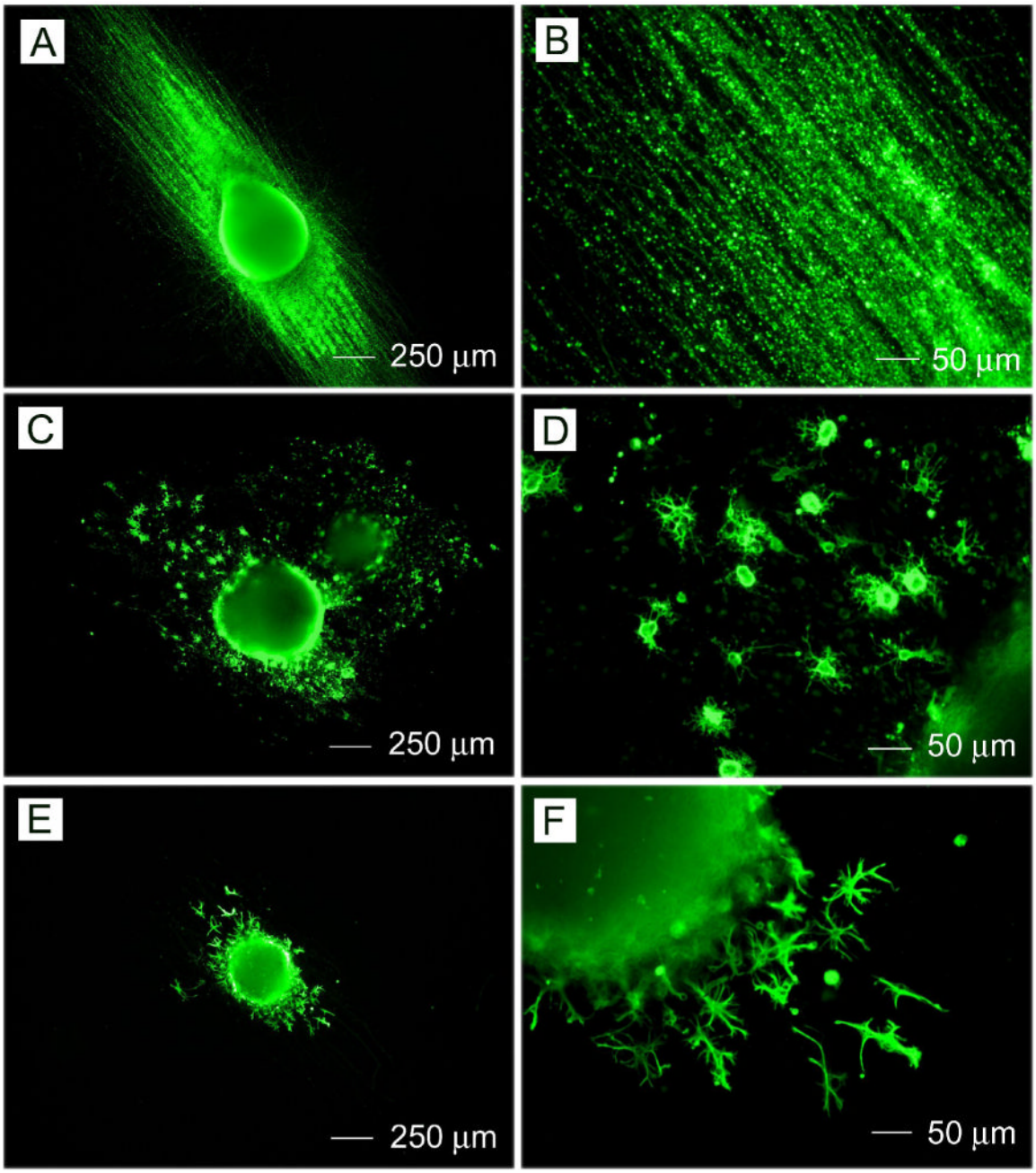

Fig.3.
Immunohistochemistry performed on RW4 EBs after 14 days of culture on aligned PCL nanofibrous for mature cell markers including (A, B) Tuj1 (for neurons), (C, D) O4 (for oligodendrocytes), and (E, F) GFAP (for astrocytes).

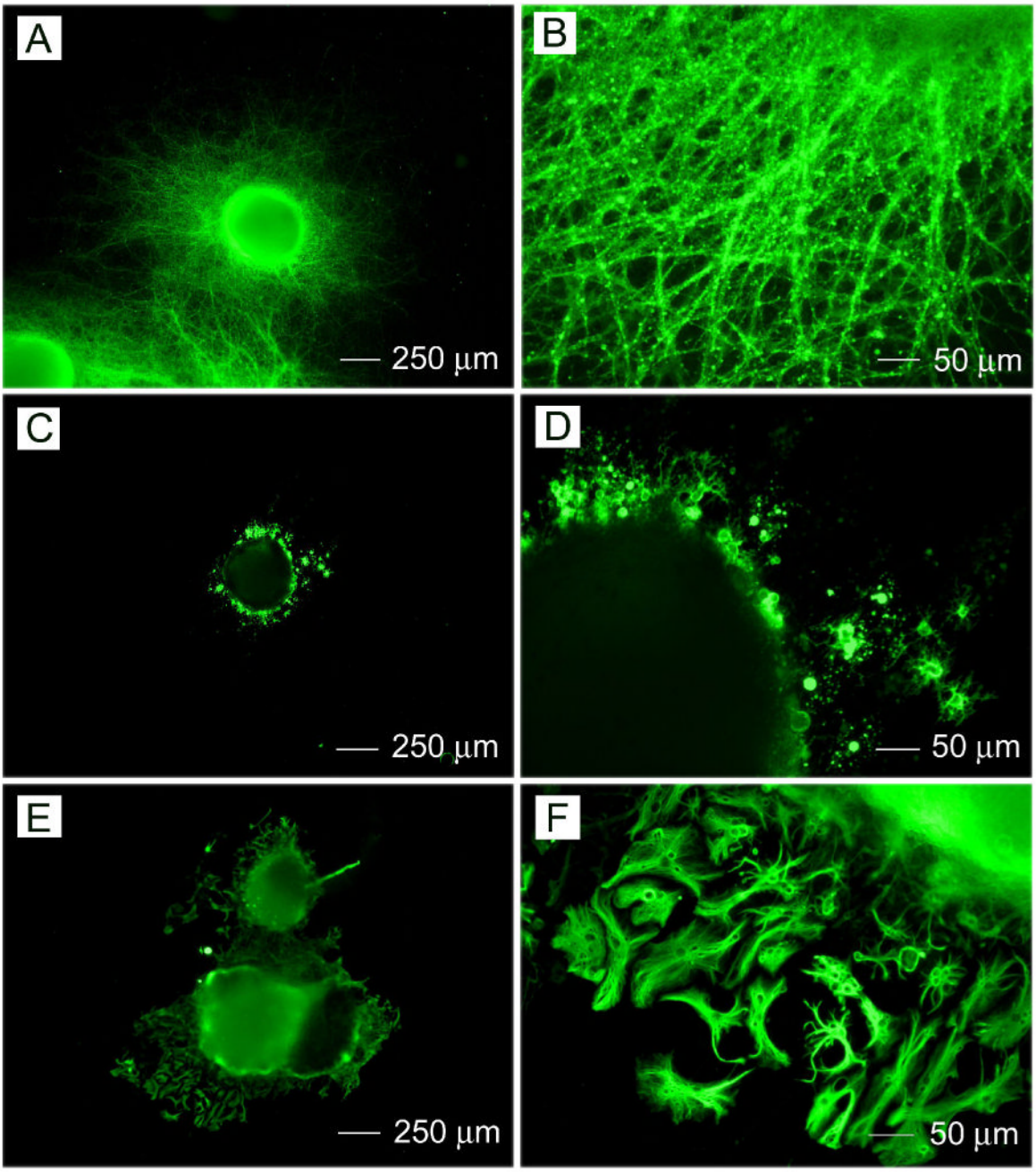

Fig.4.

Immunohistochemistry performed on RW4 EBs after 14 days of culture on randomly oriented PCL nanofibrous for mature cell markers: (A, B) Tuj1 (for neurons), (C, D) O4 (for oligodendrocytes), and (E, F) GFAP (for astrocytes).

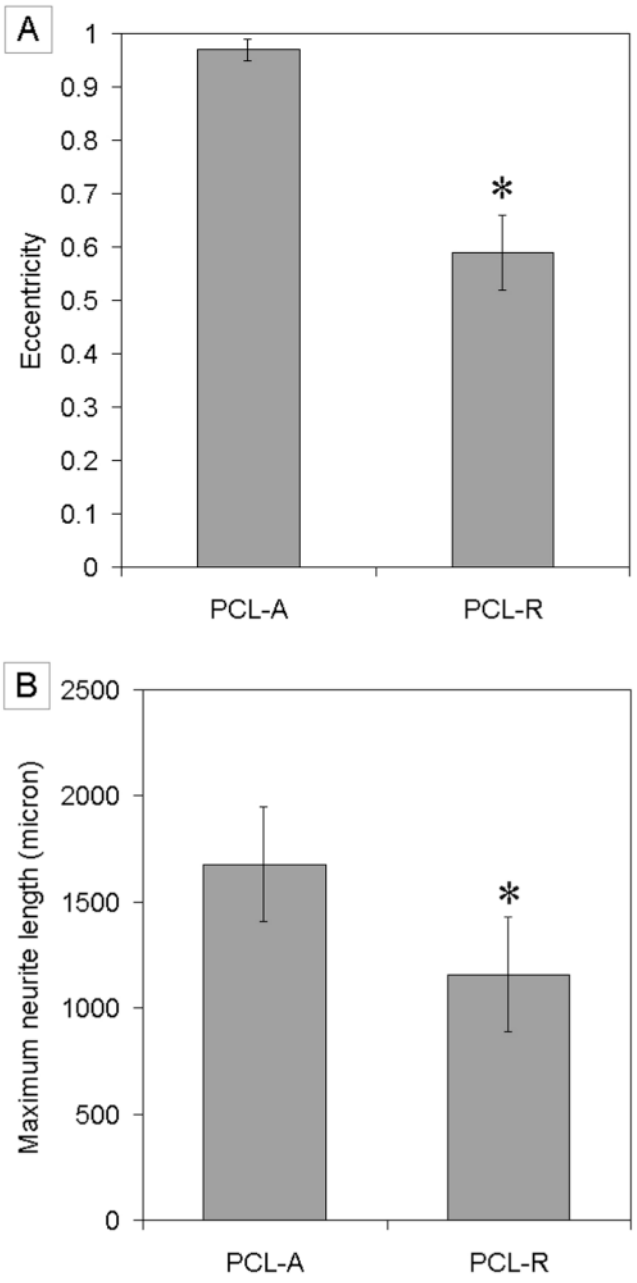

Fig.5.

A) Eccentricity of neurite field. B) Maximum neurite length. * indicates $p<0.05$ for eccentricity of neurite field on PCL-R and maximum neurite length from PCL-R as compared to eccentricity of neurite field on PCL-A and maximum neurite length from PCL-A. Abbreviations: aligned PCL nanofibers; PCL-R, random PCL nanofibers.

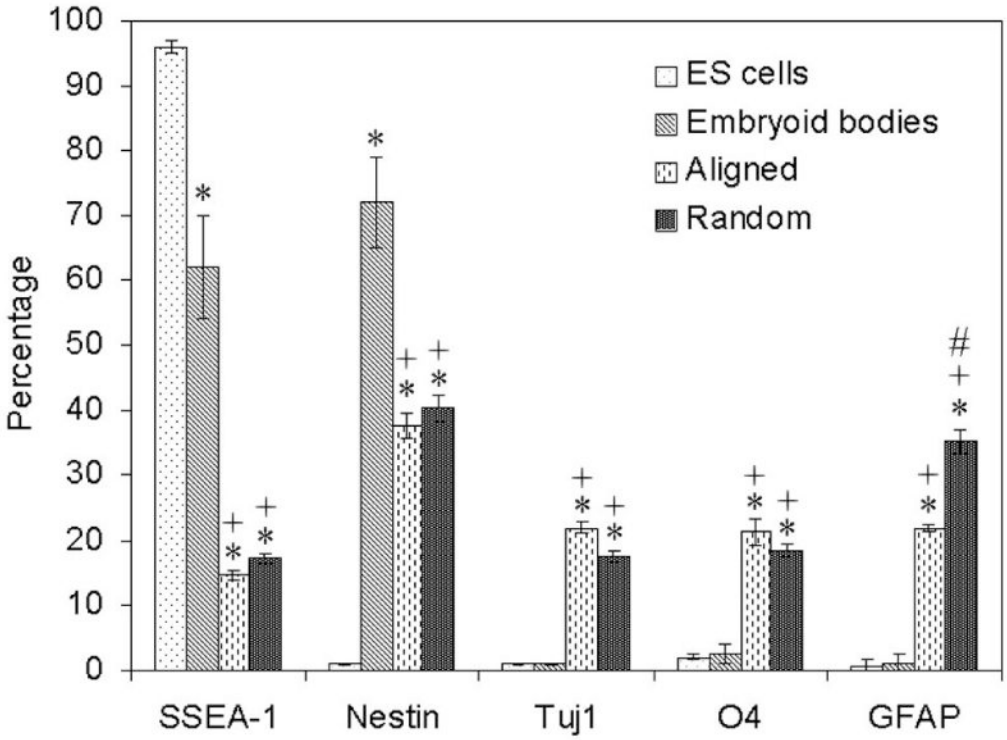

Fig.6.

Cell phenotype analysis of RW4 EBs cultured on PCL nanofibrous scaffolds for 14 days. The markers examined were SSEA-1 (for undifferentiated mouse ES cells), nestin (for neural precursors), Tuj1 (for neurons), O4 (for oligodendrocytes), and GFAP (for astrocytes). * indicates $p < 0.05$ for markers compared with embryonic stem cells. + indicates $p < 0.05$ for markers compared with embryoid bodies. # indicates $p < 0.05$ for markers compared with random PCL fibers. Abbreviations: SSEA-1, stage specific embryonic antigen; Tuj1, β-tubulin III; GFAP, glia fibrillary acidic protein.

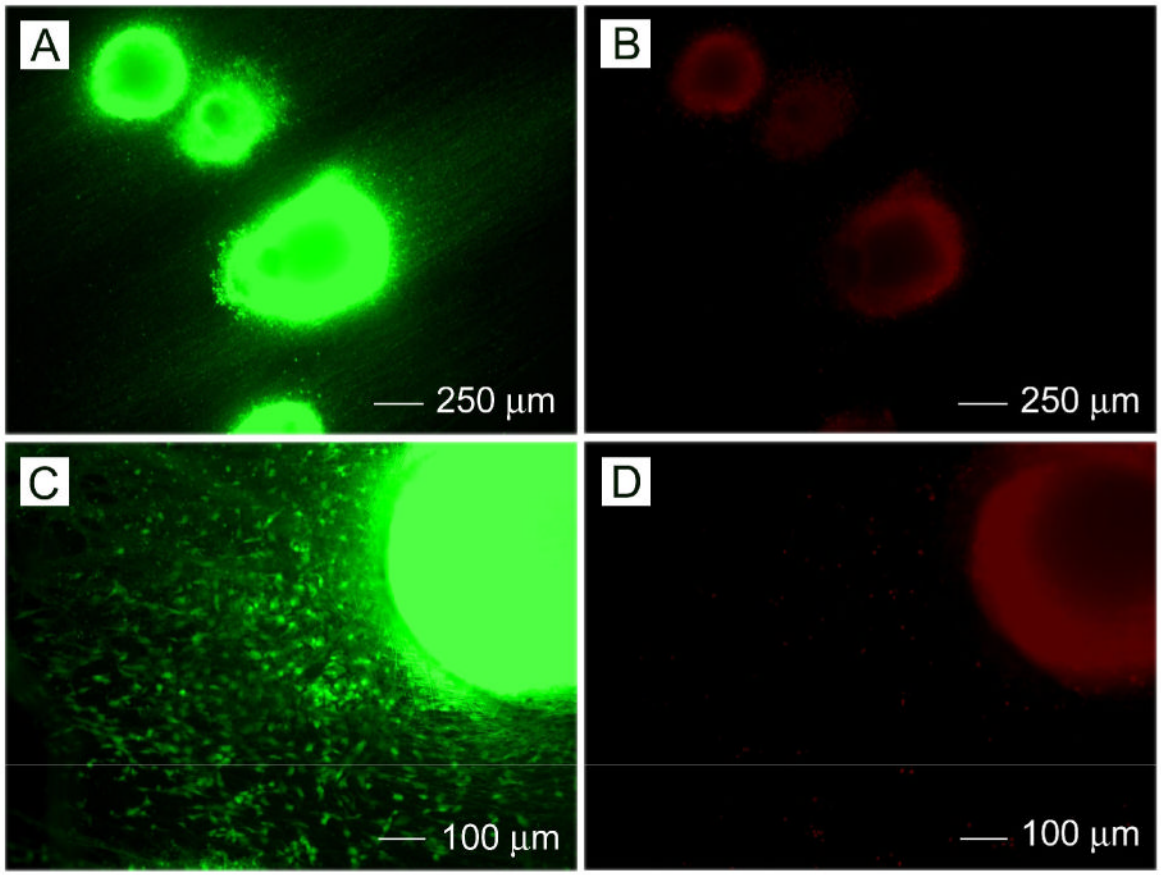

Fig.7.
(A, B) Cell viability of intact RW4 EBs seeded on aligned PCL nanofibers after 14 days of culture as determined by live/dead assay. (C, D)Cell viability of intact RW4 EBs seeded on random PCL nanofibers after 14 days of culture as determined by live/dead assay.

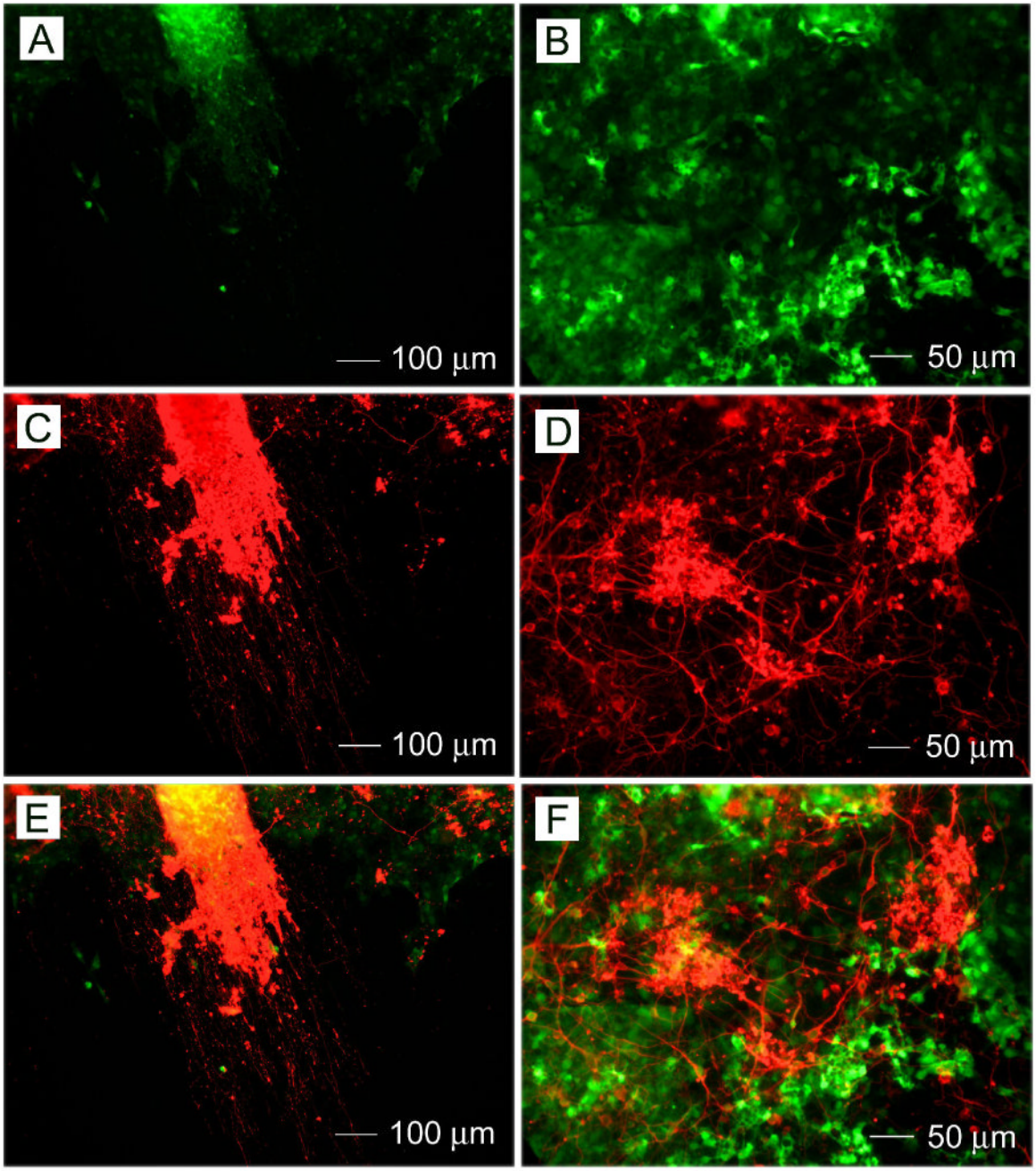

Fig.8.

Neuronal differentiation of CE3 cells seeded on (A, C, and E) aligned and (B, D, and F) random PCL nanofibers directly without forming EBs induced by retinoic acid using 4-/4+ and incubated with neurobasal medium with B27 as a supplement for 14 days. (A, B) Fluorescence micrographs of CE3 cells. (C, D)Neuron marker Tuj1 staining of the same regions as in (A) and (B). E) A superimposed image of (A) and (C). F) A superimposed image of (B) and (D).